

Monolithic integration of GaN-based light-emitting diodes and metal-oxide-semiconductor field-effect transistors

Ya-Ju Lee,^{1,*} Zu-Po Yang,² Pin-Guang Chen,^{1,3} Yung-An Hsieh,¹ Yung-Chi Yao,¹
Ming-Han Liao,³ Min-Hung Lee,¹ Mei-Tan Wang,⁴ and Jung-Min Hwang⁴

¹*Institute of Electro-Optical Science and Technology, National Taiwan Normal University, 88, Sec.4, Ting-Chou Road, Taipei 116, Taiwan*

²*Institute of Photonic System, National Chiao-Tung University, 301, Gaofa 3rd Road, Tainan 711, Taiwan*

³*Department of Mechanical Engineering, 1, Sec. 4, Roosevelt Road, Taipei 106, Taiwan*

⁴*Solid-State Lighting Systems Department, Green Energy and Environment Research Laboratories, Industrial Technology Research Institute (ITRI), Hsinchu 310, Taiwan*

*yajulee@ntnu.edu.tw

Abstract: In this study, we report a novel monolithically integrated GaN-based light-emitting diode (LED) with metal-oxide-semiconductor field-effect transistor (MOSFET). Without additionally introducing complicated epitaxial structures for transistors, the MOSFET is directly fabricated on the exposed n-type GaN layer of the LED after dry etching, and serially connected to the LED through standard semiconductor-manufacturing technologies. Such monolithically integrated LED/MOSFET device is able to circumvent undesirable issues that might be faced by other kinds of integration schemes by growing a transistor on an LED or vice versa. For the performances of resulting device, our monolithically integrated LED/MOSFET device exhibits good characteristics in the modulation of gate voltage and good capability of driving injected current, which are essential for the important applications such as smart lighting, interconnection, and optical communication.

©2014 Optical Society of America

OCIS codes: (250.3140) Integrated optoelectronic circuits; (230.3670) Light-emitting diodes; (160.6000) Semiconductor materials.

References and links

1. R. G. Hunsperger, *Integrated Optics, Theory and Technology* (Springer, 1995).
2. I. Polentier, L. Buydens, A. Ackaert, P. Demeester, P. van Daele, F. Depestel, D. Lootens, and R. Baets, "Monolithic integration of an InGaAs/GaAs/AlGaAs strained layer SQW LED and GaAs MESFET using epitaxial lift-off," *Electron. Lett.* **26**(13), 925 (1990).
3. M. E. Groenert, C. W. Leitz, A. J. Pitera, V. Yang, H. Lee, R. J. Ram, and E. A. Fitzgerald, "Monolithic integration of room-temperature cw GaAs/AlGaAs lasers on Si substrates via relaxed graded GeSi buffer layers," *J. Appl. Phys.* **93**(1), 362–367 (2003).
4. J.-W. Shi, H.-Y. Huang, J.-K. Sheu, S.-H. Hsieh, Y.-S. Wu, F.-H. Ja-Yu Lu, F.-H. Huang, and W.-C. Lai, "Nitride-based photodiode at 510-nm wavelength for plastic optical fiber communication," *IEEE Photon. Technol. Lett.* **18**(1), 283–285 (2006).
5. K. Chilukuri, M. J. Mori, C. L. Dohrman, and E. A. Fitzgerald, "Monolithic CMOS-compatible AlGaInP visible LED arrays on silicon on lattice-engineered substrates (SOLES)," *Semicond. Sci. Technol.* **22**(2), 29–34 (2007).
6. Y. J. Lee, P. C. Lin, T. C. Lu, H. C. Kuo, and S. C. Wang, "Dichromatic InGaN-based white light emitting diodes by using laser lift-off and wafer-bonding schemes," *Appl. Phys. Lett.* **90**(16), 161115 (2007).
7. Z. J. Liu, K. M. Wong, C. W. Keung, C. W. Tang, and K. M. Lau, "Monolithic LED microdisplay on active matrix substrate using flip-chip technology," *IEEE J. Sel. Top. Quantum Electron.* **15**(4), 1298–1302 (2009).
8. H. P. T. Nguyen, S. Zhang, K. Cui, X. Han, S. Fatholouloumi, M. Couillard, G. A. Botton, and Z. Mi, "p-Type modulation doped InGaN/GaN dot-in-a-wire white-light-emitting diodes monolithically grown on Si(111)," *Nano Lett.* **11**(5), 1919–1924 (2011).
9. F. G. Kalaitzakis, E. Iliopoulos, G. Konstantinidis, and N. T. Pelekanos, "Monolithic integration of nitride-based transistor with Light Emitting Diode for sensing applications," *Microelectron. Eng.* **90**, 33–36 (2012).

10. Z. Li, J. Waldron, T. Detchprohm, C. Wetzel, R. F. Karlicek, Jr., and T. P. Chow, "Monolithic integration of light-emitting diodes and power metal-oxide-semiconductor channel high-electron-mobility transistors for light-emitting power integrated circuits in GaN on sapphire substrate," *Appl. Phys. Lett.* **102**(19), 192107 (2013).
11. Z. Liu, J. Ma, T. Huang, C. Liu, and K. M. Lau, "Selective epitaxial growth of monolithically integrated GaN-based light emitting diodes with AlGaIn/GaN driving transistors," *Appl. Phys. Lett.* **104**, 09103 (2014).
12. Z. J. Liu, T. Huang, J. Ma, C. Liu, and K. M. Lau, "Monolithic Integration of AlGaIn/GaN HEMT on LED by MOCVD," *IEEE Electron Device Lett.* **35**(3), 330–332 (2014).
13. Y.-F. Wu, B. P. Keller, S. Keller, D. Kapolnek, P. Kozodoy, S. P. Denbaars, and U. K. Mishra, "Very high breakdown voltage and large transconductance realized on GaN heterojunction field effect transistors," *Appl. Phys. Lett.* **69**(10), 1438 (1996).
14. Y. Dora, A. Chakraborty, L. McCarthy, S. Keller, S. P. Denbaars, and U. K. Mishra, "High breakdown voltage achieved on AlGaIn/GaN HEMTs with integrated slant field plates," *IEEE Electron Device Lett.* **27**(9), 713–715 (2006).
15. S. T. Sheppard, K. Doverspike, W. L. Pribble, S. T. Allen, J. W. Palmour, L. T. Kehias, and T. J. Jenkins, "High-power microwave GaN/AlGaIn HEMT's on semi-insulating silicon carbide substrates," *IEEE Electron Device Lett.* **20**(4), 161–163 (1999).
16. O. I. Saadat, J. W. Chung, E. L. Piner, and T. Palacios, "Gate-first AlGaIn/GaN HEMT technology for high-frequency applications," *IEEE Electron Device Lett.* **30**(12), 1254–1256 (2009).
17. A. G. Holmes-Siedle, "Gallium nitride, a valuable semiconductor," *Nature* **252**, 434–444 (1974).
18. J. J. D. McKendry, D. Massoubre, S. Zhang, B. R. Rae, R. P. Green, E. Gu, R. K. Henderson, A. E. Kelly, and M. D. Dawson, "Visible-light communications using a CMOS-controlled micro-light-emitting-diode array," *J. Lightwave Technol.* **30**(1), 61–67 (2012).
19. E. F. Schubert and J. K. Kim, "Solid-state light sources getting smart," *Science* **308**(5726), 1274–1278 (2005).
20. K. Hazu and S. F. Chichibu, "Optical polarization properties of m-plane Al_xGa_{1-x}N epitaxial films grown on m-plane freestanding GaN substrates toward nonpolar ultraviolet LEDs," *Opt. Express* **19**(S4), A1008–A1021 (2011).
21. Y. J. Lee, H. C. Kuo, T. C. Lu, and S. C. Wang, "High light-extraction GaN-based vertical LEDs with double diffuse surfaces," *IEEE J. Quantum Electron.* **42**(12), 1196–1201 (2006).
22. T. Wei, Q. Kong, J. Wang, J. Li, Y. Zeng, G. Wang, J. Li, Y. Liao, and F. Yi, "Improving light extraction of InGaIn-based light emitting diodes with a roughened p-GaN surface using CsCl nano-islands," *Opt. Express* **19**(2), 1065–1071 (2011).
23. C. Y. Huang, Y. C. Yao, Y. J. Lee, T. Y. Lin, W. J. Kao, J. Shang Hwang, Y. J. Yang, and J. L. Shen, "Local nanotip arrays sculptured by atomic force microscopy to enhance the light-output efficiency of GaN-based light-emitting diode structures," *Nanotechnology* **25**(19), 195401 (2014).
24. J. K. Sheu, Y. K. Su, G. C. Chi, P. L. Koh, M. J. Jou, C. M. Chang, C. C. Liu, and W. C. Hung, "High-transparency Ni/Au ohmic contact to p-type GaN," *Appl. Phys. Lett.* **74**(16), 2340 (1999).
25. R. H. Horng, C. C. Yang, J. Y. Wu, S. H. Huang, C. E. Lee, and D. S. Wu, "GaN-based light-emitting diodes with indium tin oxide texturing window layers using natural lithography," *Appl. Phys. Lett.* **86**(22), 221101 (2005).

1. Introduction

The demand of monolithic integration of light-emitting diodes (LEDs) with field-effect transistors (FETs) is increased for the recent surge in smart-lighting applications, which generally involves sophisticated electronic circuit designs for the AC-DC power convertor, current source, and photo-detectors [1]. Through the monolithic integration that shares the same material platform, the fabrication cost and dimension of lighting systems can be considerably reduced, offering a great functionality and stability for a broad range of applications. Among previous successful demonstrations of monolithic integration of optoelectronic devices on various material systems [2–12], the monolithic integration of GaN-based LEDs and FETs is of research interest due to their unique material properties such as large breakdown voltage [13, 14], high operating frequency [15, 16], and high temperature duration [17], and that makes it preferable for the emerging markets of high power-high voltage lighting systems and visible light communication [18, 19]. However, there have been only few reports on the monolithic integration of GaN-based LEDs and FETs, due mainly to the restriction of realizing complicated epitaxial structures. For example, Li *et al.* reported a monolithic integration of GaN-based LED and high-electron-mobility transistor (HEMT) structure [10]. Although such LED-on-HEMT is easy to make on-chip interconnection, it would be difficult to grow high performance LED on the top of HEMT with AlGaIn epitaxial layer instead of sapphire substrates due to the lattice mismatch issue [20]. Very recently, Liu *et al.* reported a monolithic integration of GaN-based HEMT-on-LED structure, but to avoid damaging multiple quantum wells (MQWs) of LEDs

underneath, a conflicting choice of low growth temperature for HEMT might degrade its crystalline quality and result in low mobility of the transistor [11, 12]. In this study, we demonstrate a monolithic integration of GaN-based LED and metal-oxide-semiconductor (MOS) FETs. As the MOSFET is directly fabricated on the exposed n-type GaN layer of the LED after dry etching process, no additional growth of HEMT architecture is required, and that eliminates as-mentioned issues which might be arisen during epitaxial procedures. In short, our monolithically integrated LED/MOSFET device is able to circumvent undesirable issues that might be faced by other kinds of integration schemes by growing a transistor on an LED or vice versa. For the performances of resulting device, the fabricated monolithically integrated LED/MOSFET device exhibits a maximum output current of $I_{DS} = 1050$ mA/mm and a peak transconductance of $G_m = 368$ mS/mm. The LED exhibits a well rectifying behavior with a slightly high turn-on voltage of 5.32V. Its light out power is about 4.86 mW at $I = 20$ mA, which corresponds to a peak EQE value of 7.52%. Those output characteristics measured on our monolithically integrated LED/MOSFET device are compactable to that of previously reported GaN-based monolithically integrated schemes [10–12]. Additionally, such design provides a large flexibility and feasibility for on-chip interconnection and optical modulation since the cathode of the LED and the drain of the MOSFET are electrically connected. As a result, we believe the proposed integration structure is viable and highly promising for smart-lighting applications.

2. Experiment

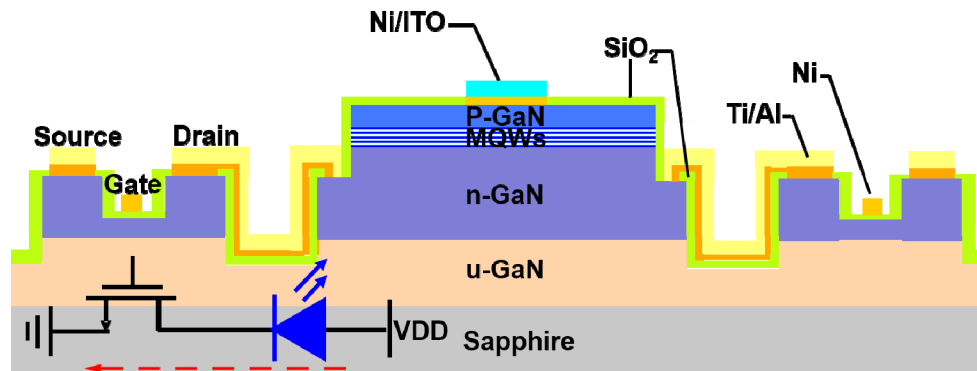


Fig. 1. Schematic plot of monolithically integrated GaN-based light-emitting diode (LED) and metal-oxide-semiconductor field-effect transistor (MOSFET) device. The equivalent electronic circuit of monolithically integrated LED/MOSFET device is also inserted in the figure.

Figure 1(a) shows a schematic configuration of monolithic integration of GaN-based LED and MOSFET. An LED structure was grown onto 2-inch sapphire substrates using a low-pressure metal-organic chemical vapor deposition (Aixtron 2600G) system. The LED layer-structure comprised of a 30-nm-thick GaN nucleation layer grown at 520°C, a 2- μ m-thick undoped GaN layer grown at 1050°C, 2- μ m-thick Si-doped n-type ($n = 5 \times 10^{18}$ cm⁻³) GaN cladding layer grown at 1050°C, an unintentionally doped active region of five periods InGaN/GaN MQWs grown at 700 °C with emitting wavelength of $\lambda = 485$ nm, and a 200-nm-thick Mg-doped p-type ($p = 3 \times 10^{17}$ cm⁻³) GaN layer grown at 800°C. The low growth temperature of p-type GaN layer is to roughen its surface for enhanced light extraction efficiency of the LED [21–23]. The LED structure was then selectively removed by dry etching (inductively coupled plasma, ICP) with Ar/Cl₂ mixed gases to expose the n-type GaN layer for the subsequent fabrication of MOSFET. A 2- μ m-deep trench down to the undoped GaN layer was created to isolate the LED and MOSFET mesa regions by an additional ICP process. A 500-nm-thick SiO₂ passivation layer was then deposited on the sidewalls of LED and MOSFET mesas by plasma-enhanced chemical vapor deposition (PECVD). Next, the

remaining of n-type GaN layer on top of the MOSFET mesa was patterned by standard photolithography and ICP dry etching that gives a film of 150 nm for the current channel. After that, a 200-nm-thick SiO₂ layer was deposited as a gate dielectric by using PECVD again at an operating temperature of 300°C. Ti/Al was deposited by e-beam evaporation and annealed by rapid thermal annealing (RTA) at 600°C for 30sec in N₂ ambient for source/drain contact metals of the MOSFET and cathode of the LED. ITO/Ni was deposited by the RF magnetron sputtering, patterned by lift-off process, and annealed at 450°C for 2 minutes in O₂ ambient to form p-type ohmic contacts for the LED. Finally, Ni was deposited and patterned as the gate electrode of the MOSFET.

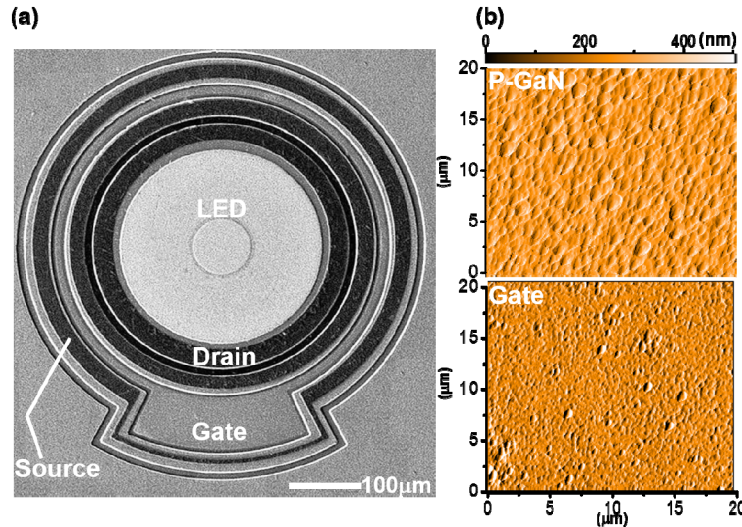


Fig. 2. (a) Top-view SEM image of the monolithically integrated and serially connected LED/MOSFET device. (b) AFM images of the LED (top, p-GaN region) and MOSFET (bottom, Gate region) surfaces with a scanned area of $20 \times 20 \mu\text{m}^2$.

Figure 2(a) shows the top-view scanning electron microscope (SEM) image of our monolithically integrated LED/MOSFET device. Accordingly, as the LED mesa is surrounded by the MOSFET, the electron flow (originated from the source terminal) injecting into the cathode of LED is uniform and well controlled, and switched by biased gate voltage, so is the LED's light output power. Additionally, such a serially connected integration provides a much compact and promising way for the subsequent fiber coupling for the application of optical communication. Figure 2(b) shows the atomic force microscope (AFM) images of the LED (top, p-GaN) and MOSFET (bottom, Gate) surfaces with a scanned area of $20 \times 20 \mu\text{m}^2$. The root mean square (RMS) estimated for the LED and MOSFET are 67.49 and 8.16 nm, respectively. As mentioned above, we intentionally roughened the LED's surface by creating inverted hexagonal pits to enhance the guided light extraction efficiency, and that causes its relatively large surface roughness on the p-GaN layer. After dry etching as shown in the bottom of Fig. 2(b), the roughness of the exposed surface of MOSFET device became smoother by an appropriate modification of ICP condition, providing a suitable platform for the subsequent PECVD growth of gate dielectric and is also beneficial to low leakage current characteristics.

3. Results and discussion

We first examine the DC characteristics of the fabricated device. Figure 3(a) shows output I_D - V_D measurements of the monolithically integrated LED/MOSFET device with the applied gate voltage (V_{GS}) ranging from $V_{GS} = -1.5\text{V}$ to 2V in 0.5V interval. The maximum output current of $I_{DS} = 1050 \text{ mA/mm}$ is achieved under $V_{GS} = 2\text{V}$, and the specific on-resistance

(R_{on}) is estimated to be $R_{on} = 105\Omega$. The output characteristic of the MOSFET is comparable to that of previously reported monolithically integrated structures based on GaN-based HEMT devices [10–12]. Figure 3(b) shows the transfer characteristics of the MOSFET for the applied source-to-drain voltage of $V_{DS} = 2V, 4V,$ and $6V$. The MOSFET exhibits a peak transconductance of $G_m = 368\text{ mS/mm}$ at $V_{DS} = 6V$, and achieves an OFF-state drain leakage current as low as $I_{off} = 2.47 \times 10^{-5}\text{ mA/mm}$ at $V_{DS} = 2V$. The DC characteristic shown in Fig. 3 suggests that the performance of the MOSFET is acceptable, and hence can be monolithically integrated with the LED device. It shall be addressed again that the MOSFET was fabricated on the exposed n-GaN layer after dry etching, and no additional growth layers of HEMT was employed in this study. Thus such device structure of monolithically integrated LED with MOSFET is more direct and also feasible without introducing other undesirable issues as previously reported in the literatures.

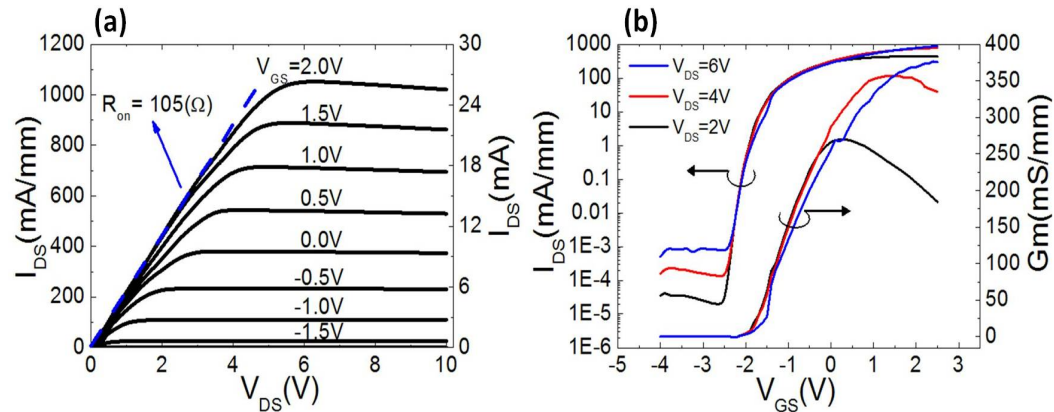


Fig. 3. (a) Output I_D - V_D and (b) transfer characteristics measured on the monolithically integrated LED/MOSFET device.

Figure 4(a) shows measured current versus voltage (I - V) curves of the LED in both linear (red line) and semi-log (black line) scales. An optical image of the fabricated device with lighted up LED at an injection current of 20mA is also inserted in the figure. Because of the absence of current spreading layer on the top of LED, a current crowding effect was clearly observed on the optical image. Nevertheless, the LED's I - V curve still exhibits a well rectifying behavior with a turn-on voltage of 5.32V, slightly higher than that of typical GaN-based blue-light LEDs due mainly to the un-optimized condition of p-contact metals (ITO/Ni) used in this study, and that could be further improved by substituting it to more generally adopted ohmic contacts metals such as Ni/Au films [24]. For the same reason, the series resistance of the LED estimated to be $R_S \sim 60.85\Omega$ is also higher than the typical value. The leakage current in the order of $2.05 \times 10^{-6}\text{ A}$ at -5 V is measured, which corresponds to a LED's shunt resistance of $R_P \sim 5.27\text{ M}\Omega$, which is acceptable for the LED with a chip size of $300\text{ }\mu\text{m}$ in diameter. Figure 4(b) plots the light output power (LOP) and external quantum efficiency (EQE) versus the injected current of the LED. The emission spectrum under the injection current of 20 mA is also inserted in the figure. The LED's light output power increases rapidly at low injected current ($I < 20\text{mA}$), and becomes saturated at higher injected currents ($I > 90\text{mA}$). The LED's EQE therefore achieves its highest value at low injection current, and then decreases pronouncedly with a further increasing of injection current. The possible reason responsible for the EQE droop in the high current could be attributed to the current crowding effect as observed on the inset of Fig. 4(a). The current crowding effect of the LED can be alleviated by the employment of the current spreading layer such as ITO films [25]. It shall be addressed here that as compared to that of the commercial available LED device, the relatively lower LOP and EQE values measured on our sample are mainly due to the un-optimized condition of p-contact metals and the absent

of current spreading layer deposited on the LED's top surfaces. Nevertheless, it will not affect the emission modulation capability of our monolithically integrated LED/MOSFET device much. Further optimization of metal contact and employment of current spreading layer to alleviate the EQE droop and to enhance the LED's I - V characteristics will be performed.

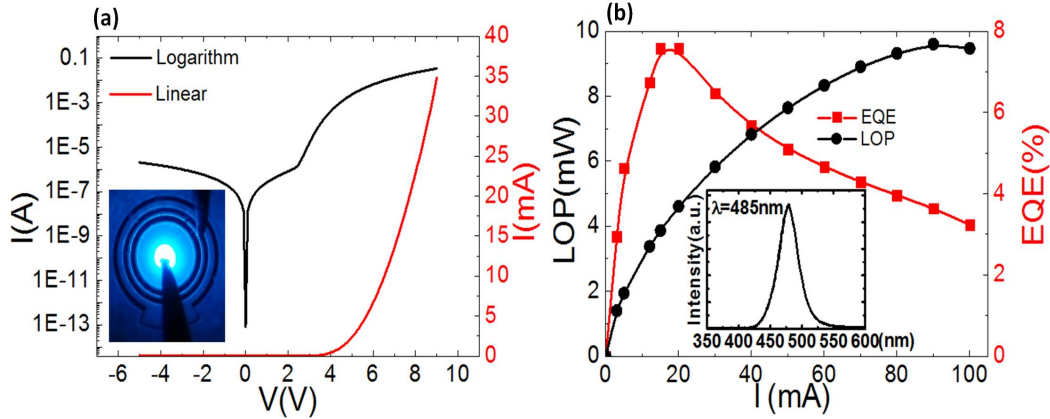


Fig. 4. (a) Current vs. voltage (I - V) behavior of the LED in both linear (red line) and semi-log (black line) scales. Inset: An optical image of the monolithically integrated LED/MOSFET device lighted up under an injection current of 20 mA. (b) Light output power (LOP) and external quantum efficiency (EQE) vs. forward injected current of the LED. Inset: EL spectrum of the LED at an injection current of 20mA with an emitting wavelength of $\lambda = 485$ nm.

Next, we are able to test the performance of the monolithically integrated LED/MOSFET device. Figure 5(a) shows LED's current (same as the source-to-drain current, I_{DS}) and light output power (LOP) versus supply voltage across the entire device (V_{DD}) for different gate voltages ranging from $V_{GS} = -1$ V to 1V in 0.5V interval. Due to the serially connected configuration between the LED and MOSFET devices (as the equivalent electrical circuit plotted in the inset of Fig. 1), I_{DS} is therefore restricted by the LED before its turn-on, and becomes saturated and dominated by the channel current of MOSFET while further increasing V_{DD} . Obviously, by a simple control of the MOSFET's V_{GS} , we are able to modulate the injected current and light output power of the LED with good linearity. As shown in the inset of Fig. 5(a), we demonstrate a LED light-switch (red line) with an ON/OFF frequency of 10kHz by directly modulating the V_{GS} of the MOSFET (black line) and the I_{DS} injected into the fabricated device (blue line). Similarly, Fig. 5(b) shows I_{DS} and LOP versus V_{GS} of the monolithically integrated LED/MOSFET device for the supply voltage of $V_{DD} = 7$ V and $V_{DD} = 15$ V. Again, the saturation of I_{DS} and LOP observed on the operating condition of $V_{DD} = 7$ V is mainly due to the limited current within the MOSFET channel. By increasing the supply voltage to a larger value of $V_{DD} = 15$ V, both I_{DS} and LOP increases linearly with the increasing of V_{GS} . Observations in Fig. 5 indicates that our monolithically integrated LED/MOSFET device exhibits good characteristics of gate controllability and current driving capability, which are essential for various applications such as smart lighting, interconnection, and optical communication.

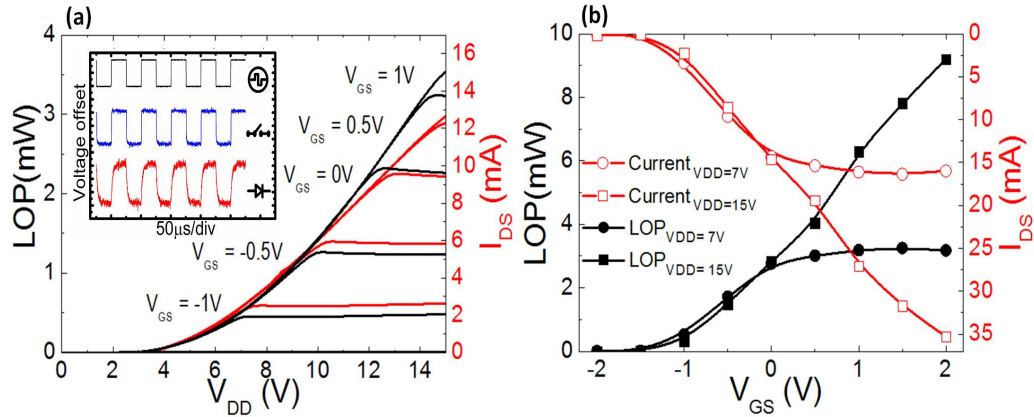


Fig. 5. (a) LED's current (same as the source-to-drain current, I_{DS}) and light output power (LOP) versus supply voltage (V_{DD}) with different gate voltages. Inset: oscilloscope signals of V_{GS} , V_{DS} , and LOP (grabbed by the photo-detector), from top to the bottom, respectively. (b) I_{DS} and LOP versus V_{GS} for both $V_{DD} = 7V$ and $V_{DD} = 15V$.

4. Conclusion

In conclusion, we have demonstrated a monolithic integration of optoelectronic (LED) and electronic (MOSFET) devices in the GaN-based platform by using standard semiconductor-manufacturing technologies. The fabricated monolithically integrated LED/MOSFET device exhibits a maximum output current of $I_{DS} = 1050$ mA/mm and a peak transconductance of $G_m = 368$ mS/mm. The LED exhibits a well rectifying behavior with a slightly high turn-on voltage of 5.32V, mainly due to the un-optimized condition of p-contact metal. Most importantly, the monolithically integrated LED/MOSFET device exhibits good gate controllability in the LED's light output power, and hence is viable and highly promising for a broad range of applications.

Acknowledgments

The authors gratefully acknowledge financial support from the Ministry of Science and Technology in Taiwan (contracts No. MOST 103-2112-M-003-008-MY3 and NSC 102-2218-E-009-017), and from the Bureau of Energy, Ministry of Economic Affairs in Taiwan.